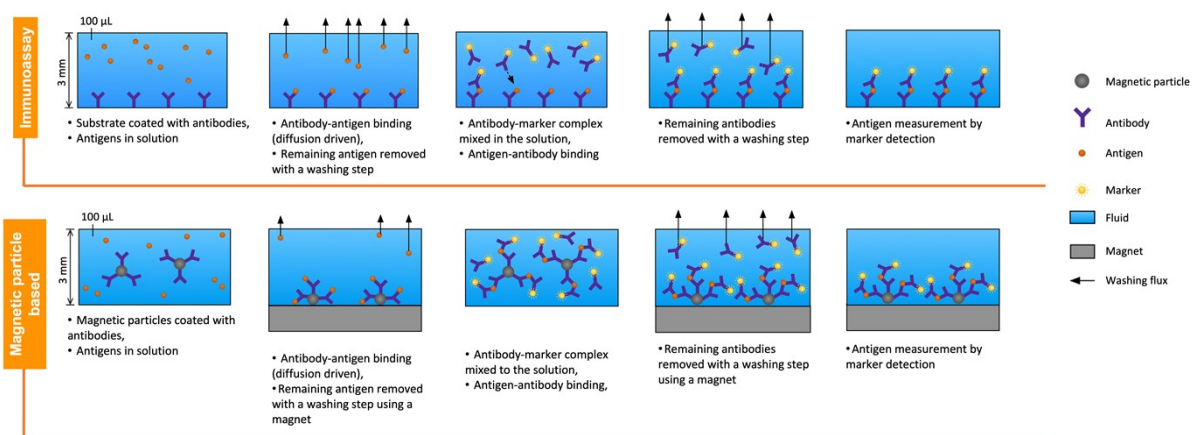


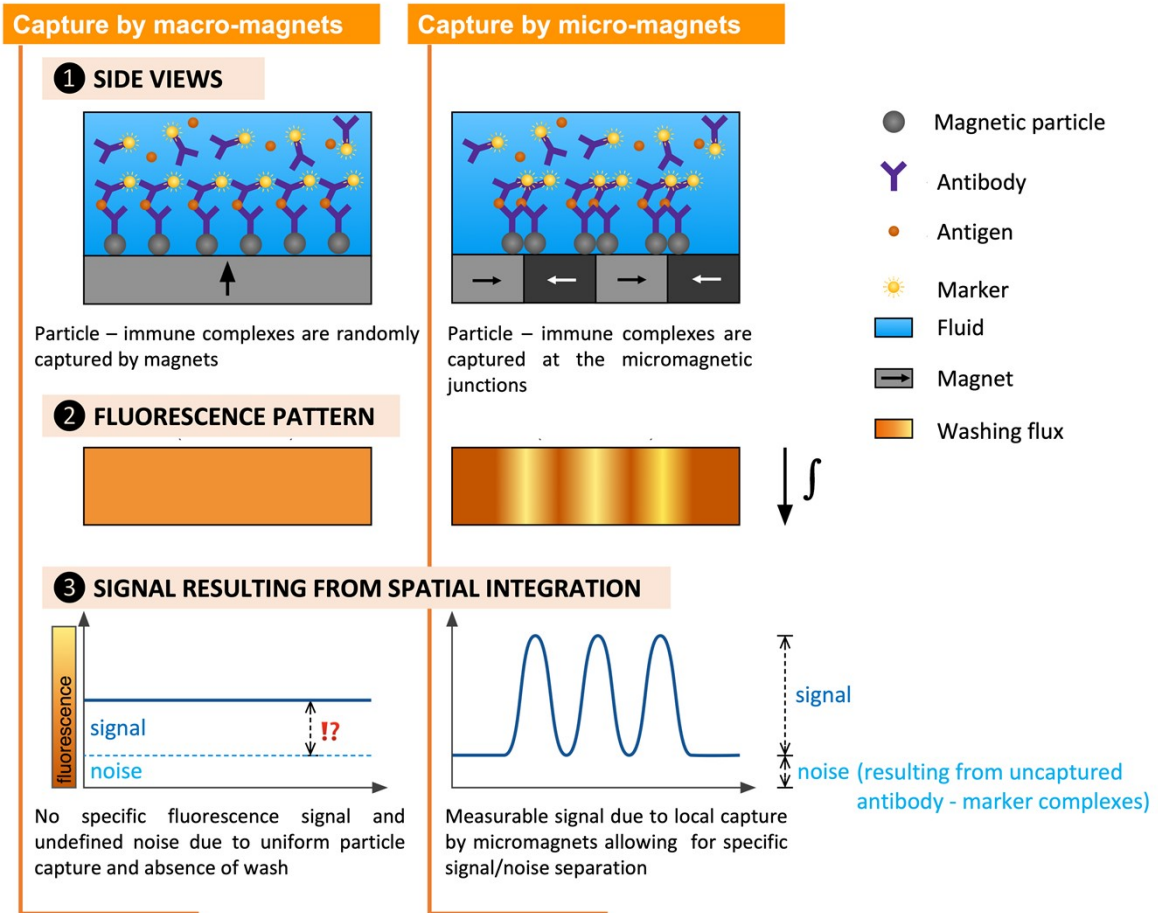
Magnetically Localized and wash-free Fluorescent Immuno-Assay (MLFIA): proof of concept and clinical applications

Delshadi S. et al.

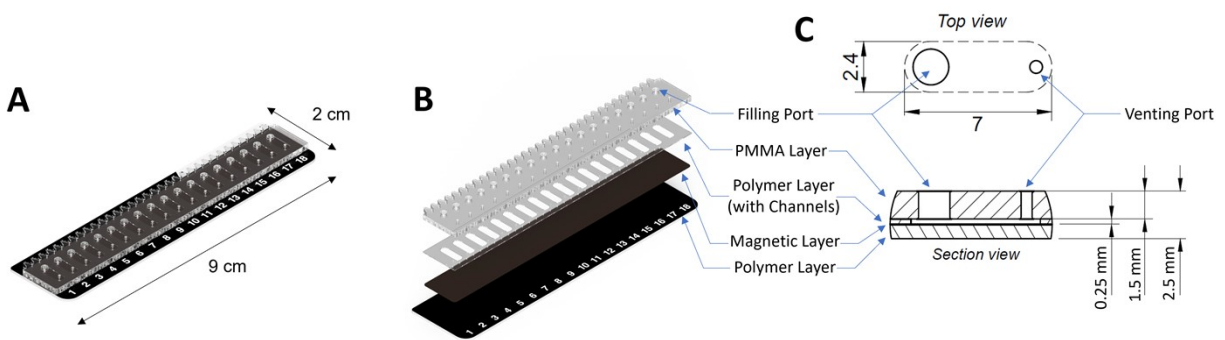
Supplementary Material



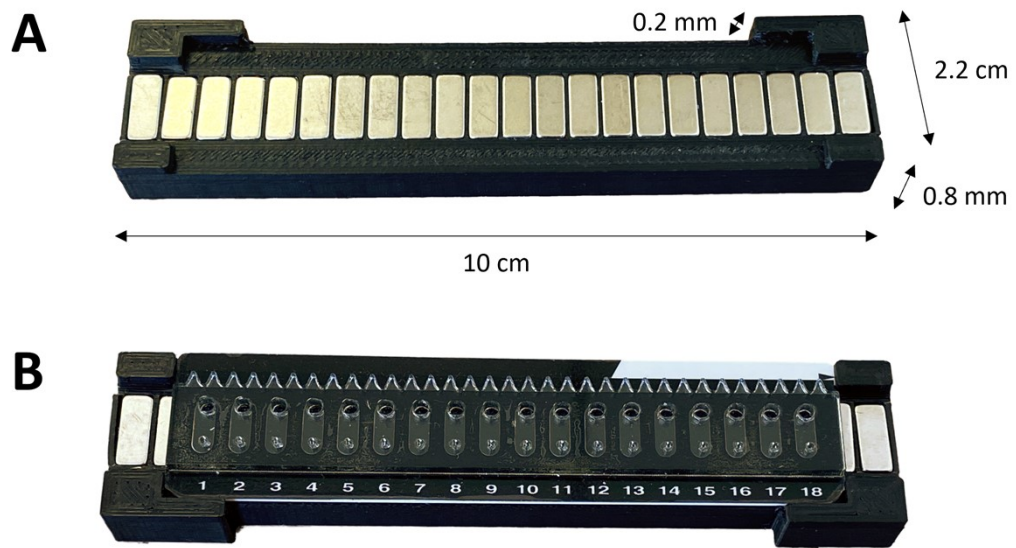
Supp. Figure 1: Conventional immunoassay, with probes grafted on a solid and fixed substrate, versus magnetic particles-based immunoassay, with probes grafted on a mobile substrate. (Top) In a conventional ELISA, the solution to be analyzed, often diluted serum, is added to a micro-well. The micro-well surface was previously functionalized with capture antibodies and saturated with inert protein. If the antigen to be detected is present in the solution, it will diffuse towards the antibodies and bind specifically to them. Then 3-5 washing steps are conducted to eliminate the unbound antigen and the supernatant. To visualize the amount of captured antigen, a second antibody coupled to marker is used. 3-5 washing steps are carried out to eliminate the unbound antibody. The quantity of marker after washing is proportional to the quantity of antigen to detect. [1]. (Bottom) In a magnetic immunoassay, magnetic particles provide a faster reaction (with a reaction in liquid volume) and more binding surface, magnets facilitate the washes, with the magnetic particles and immune complexes immobilized on the magnet surface.



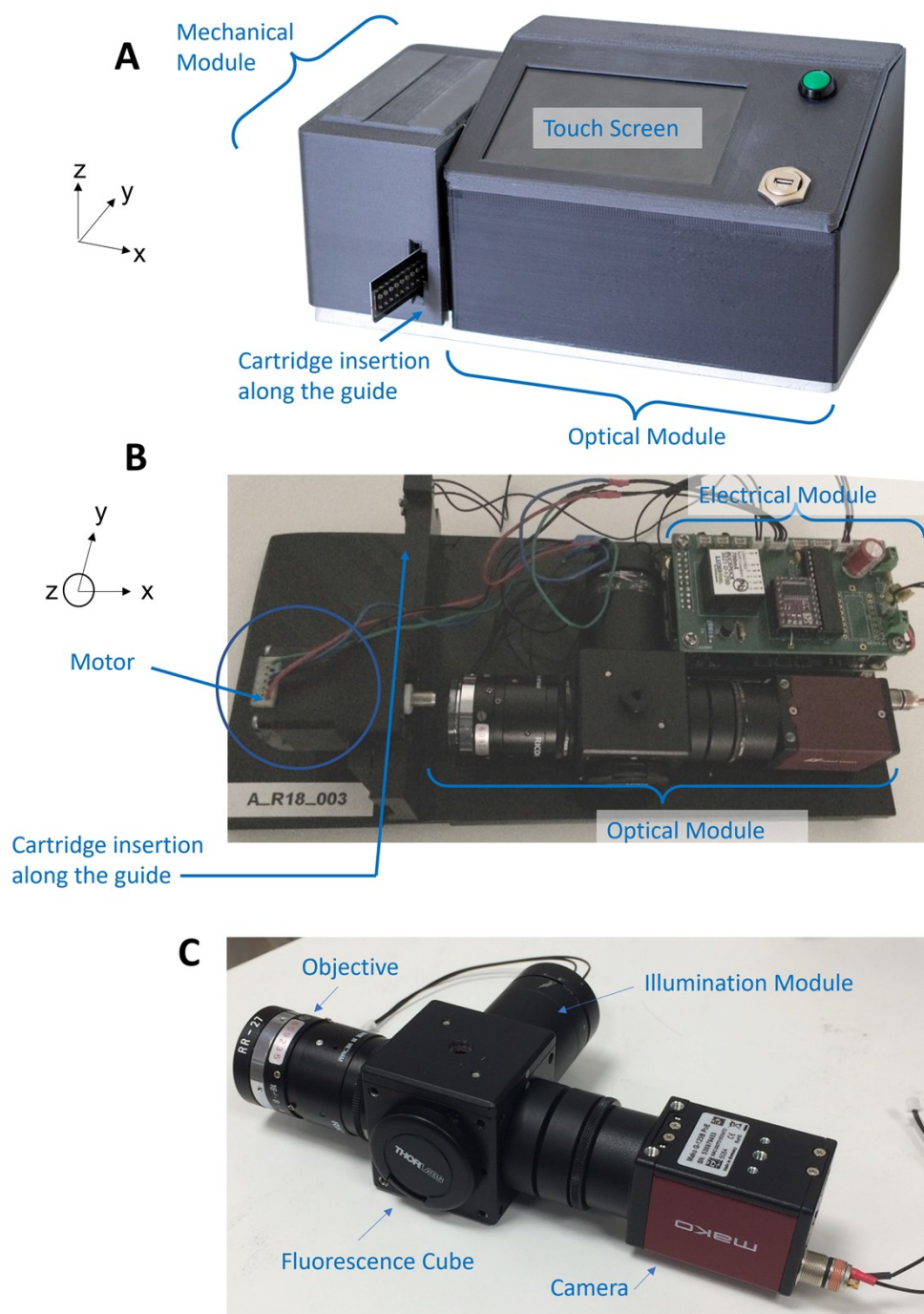
Supp. Figure 2: Capture with a macro magnet versus micro-magnets. The local capture of immune complexes at the junction of micro-magnets enables for a distinct specific signal of immune complexes and noise (fluorescent background) separation and a downstream quantification of the signal.



Supp Figure 3: (A) Presentation of the assembled MLFIA cartridge with 18 chambers. (B) Exploded view of the Cartridge and its different layers. (C) Schematic representations – top and section views - of one chamber and its different layers, with the dimensions in mm.



Supp. Figure 4: Description of the MagActivator. (A) The MagActivator is composed of 22 rectangular magnets (10 x 4 x 1 mm), assembled head-to-tail in a 3D printed black support, with the dimensions provided. (B) Cartridge positioning on the MagActivator, on top of the series of magnets.



Supp Figure 5: (A) Presentation of the Analyzer in its enclosed 3D printed box. (B) Inside view of the Analyzer and its different parts: the optical system, the mechanical system, and the electrical components. The blue arrow indicates where the cartridge is inserted. The blue circle highlights the motor that allows the automatic displacement of the cartridge for its visualization by the optical module. (C) Optical components.

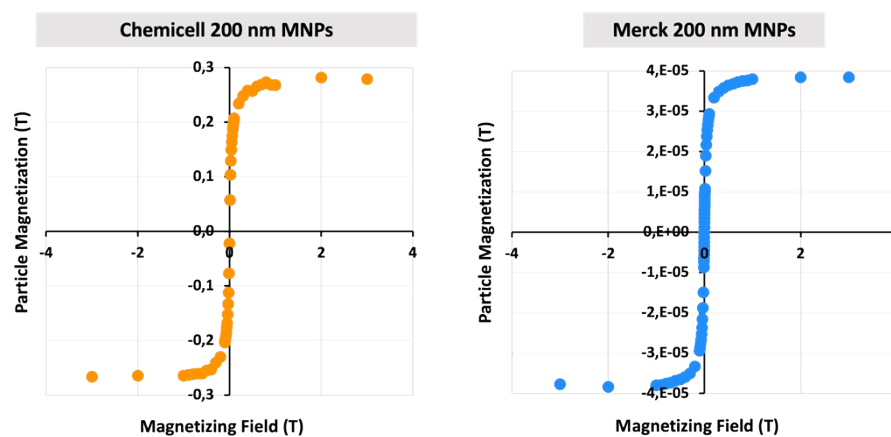
A

	Nano Particles	Micro Particles
Diameter (m)	2×10^{-7}	1×10^{-6}
Diffusion ($m^2 \cdot s^{-1}$)	2.2×10^{-12}	4.40×10^{-13}
Sedimentation velocity ($m \cdot s^{-1}$)	5.45×10^{-9}	4.36×10^{-7}
Percentage of sedimentation after 5 min.	0.02 %	2.04 %
Percentage of sedimentation after 50 min.	0.2 %	20 %

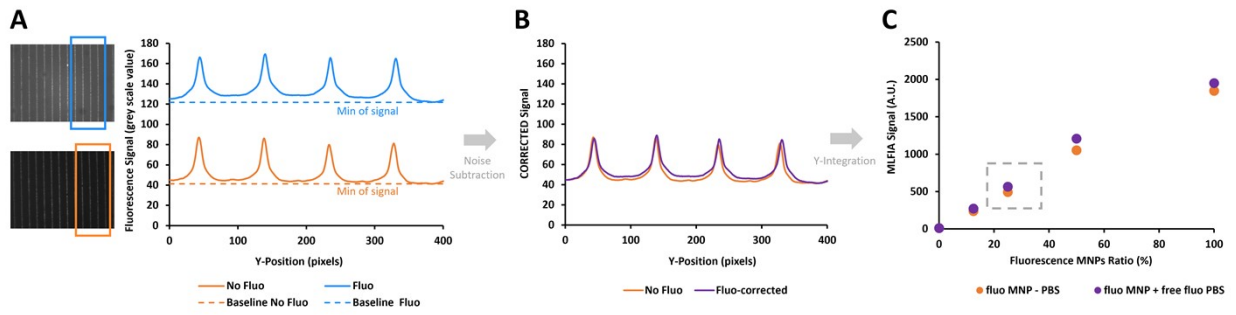
B

MNP coating	Protein A or protein G	Streptavidin	COOH
Compatible Molecules	Antibodies	Biotinylated molecules	Amine functions
Functionalization Time	Very fast	Fast, but requires biotinylation	Fast
Binding Quality	++	++++	+++ (covalent)

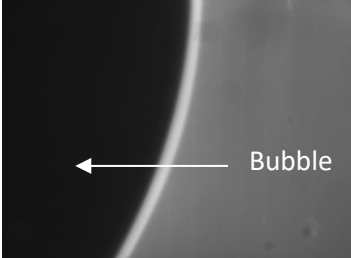
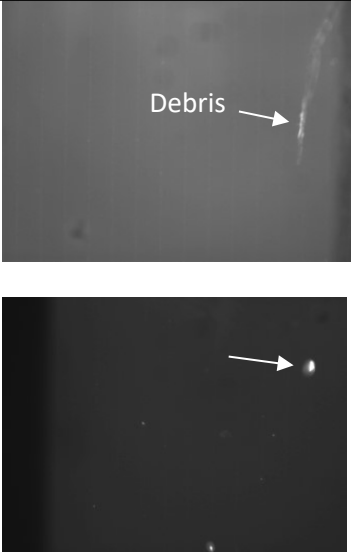
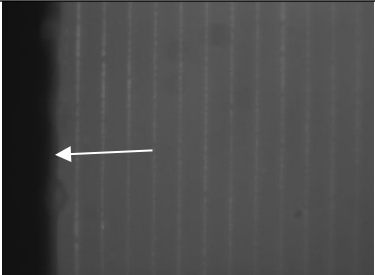
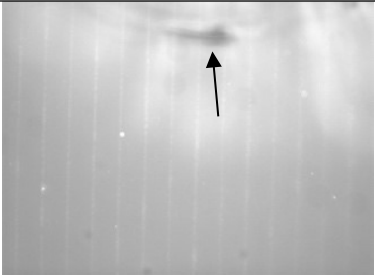
Supp. Figure 6: (A) Particle coating options. (B) Comparison of diffusion and sedimentation for magnetic nano and micro particles, with a diameter of 200 nm and 1 μ m respectively.



Supp. Figure 7: Magnetic characterization of the MNPs (at -10°C) with an extraction magnetometer indicates the absence of a remanent magnetization, thus confirming their superparamagnetic behavior (left, Chemicell and right, Merck MNPs respectively).



Supp Figure 8: Illustration of the Wash-free concept. (A) Images obtained for 25% Fluorescent MNPs in PBS (orange curve) and for 25% Fluorescent MNPs in PBS with free fluorescence (blue curve). (B) The purple curve is obtained by subtracting the difference between the minima of the blue and orange curves. (C) After Y-integration, we obtain the exact same MLFIA signal, with (purple) or without (orange) an initial free fluorescence in the reaction mix to be analyzed. This confirms that our no-wash algorithm works wells, i.e. enables the fluorescent background subtraction to identify the signal of interest.

Cause (A): Presence of artifacts causing undesired fluorescence heterogeneity.		
		
#1: Fluorescence heterogeneity caused by a bubble created during the cartridge filling. Our code takes the bubble into account, but we still lose 50% of the signal.	#2 and 3: Fluorescence heterogeneity caused by aggregates, dusts or debris brought onto the cartridge during its manual assembly.	#4: Fluorescent cloud resulting from a mixing issue.
Cause (C): Cartridge optical misalignment.		Cause (D): Focusing.
		
#5: Optical cartridge misalignment leading to the presence of the chamber edge in the picture – causing a signal loss.	#6: Optical cartridge misalignment leading to the presence of the injection well – causing a fluorescence pattern inhomogeneity.	#7: The focus is suboptimal; the image is blurry, resulting in a loss of signal.

Supp. Table 1: Cartridge variability issues – localized with arrows - and examples.

Cause (A): Presence of artifacts on the image, such as bubbles, aggregates, or debris. These artefacts cause undesired fluorescence heterogeneity.

- The bubbles can be well filtered by the algorithm but still decrease the overall signal (see picture #1). Bubble formation could be avoided by modifying the hydrophobicity of the substrate and/or optimizing the fluidic filling with the future automated instrument.

- Fluorescent aggregates, however, might be not OR partially OR incorrectly taken into account, depending on their origin. Pictures #2 and 3 represent vertical fluorescence inhomogeneities or localized variations, which would be typically considered as specific by our code and would artificially increase the signal. These inhomogeneities are dusts or debris brought onto the cartridge during its

manual assembly. These could be avoided by a cartridge assembly fully set-up in a clean room environment.

- Picture #4 corresponds to another kind of artefact: a fluorescent cloud. Such fluorescence agglomerate could be resolved by adding a mixing module in our next instrument iteration.

Cause (B): Abnormal capture pattern. Although the MagActivator has been designed to generate a homogenous magnetic field across the cartridge, the manual positioning of the cartridge on the MagActivator may not be perfect and can generate a variation in the capture.

Cause (C): Misalignment of the cartridge with respect to the optical axis, resulting from the imprecision of the manual cartridge assembly. Such optical misalignment leads to the unexpected presence of the chamber edge in the picture (see picture #5) – causing a signal loss – or the presence of the injection well (see picture #6) – causing a fluorescence inhomogeneity. Such misalignment issue will be addressed with a better controlled assembly line for the cartridge.

Cause (D): Variation of the optimal focus, from a cartridge to another. Because our cartridge fabrication is still manual, not all cartridges are strictly similar. This implies an inherent risk of cartridge misalignment, and the need for manual focusing adjustment. A suboptimal focus leads to a loss of signal (see picture #7). Such issue could be resolved with a robust fabrication process, tight dimension tolerance, and a focusing quality control implemented in the future imaging instrument.

Supp. Material – References

[1] D. Wild, 2013, *The Immunoassay Handbook: Theory and Applications of Ligand Binding, ELISA and Related Techniques*. Editions Newnes.